Polymer Bulletin 36, 355–360 (1996)

Polymer Bulletin

The effect of melting point distributions on DSC melting peaks

C. J. G. Plummer*, H.-H. Kausch

Laboratoire de Polymères, Ecole Polytechnique Fédérale de Lausanne, CH-1015, Switzerland

Received: 13 October 1995/Accepted: 6 November 1995

Summary

We have investigated the influence of scanning rate on the form of DSC melting curves in semicrystalline polymers in which the melting point varies spatially within the sample. A numerical solution for the heat balance in the sample cell was used, taking into account heat absorbed during the melting transition for a given sample mass. The simulation accounted well for the effects of scanning rate on the shape of the DSC peak for polyoxymethylene samples crystallized above 150 °C, which were assumed to be free from effects arising from lamellar thickening during the scan.

Introduction

Semicrystalline polymers differ from pure metals, for example, in that they do not normally exhibit a single well defined melting point, T_m. T_m depends instead on the crystallization conditions, which determine the lamellar thickness distribution. For a lamellar thickness l, it is generally assumed that

$$T_m = T_{mo}(1 - 2\sigma_e/l\Delta h) \quad \ldots (1),$$

where T_{mo} is the equilibrium melting point, Δh is the heat of fusion per unit volume and σ_e is the fold surface energy. By using differential scanning calorimetry (DSC) to measure the distribution of T_m one might thus hope to obtain an idea of the distribution of l in a given sample (1-5). Apart from the tendency of semicrystalline polymers to recrystallize or undergo lamellar thickening during DSC heating scans, DSC output is sensitive to the test conditions and the calibration method employed. In what follows we present a method for evaluating the quantitative influence of variations in l by simulating the DSC melting peak for a given distribution of T_m. DSC data for polyoxymethylene (POM) are then briefly discussed in terms of the model.

Experimental

Calorimetry was carried out under dry N_2 using the Perkin Elmer DSC7. The temperature scale was calibrated by extrapolating measured T_m for metal standards to zero scanning rate, and the heat transfer coefficient between the furnace and the sample holder, γ, was obtained

* Corresponding author

from indium melting peaks as discussed elsewhere (6). The POM was a non-commercial grade with M_W = 42,000 and a polydispersity of approximately 2, and contained an unspecified nucleating agent. Here we considered only crystallization temperatures, T_c, greater than 150 °C (in POM, the position of the DSC melting peak is found to be independent of T_c for T_c < 150 °C, suggesting extensive lamellar thickening during the scan (7), an effect which we wished to avoid). Films of about 70 μm in thickness were moulded at 200 °C using a miniature press. Discs with the same diameter as the DSC sample pans were cut from the films, remelted in the DSC at 185 °C and crystallized isothermally at 153 °C for 5 minutes. They were then held at 150 °C for 1 minute and subjected to a constant positive heating rate scan up to 185 °C.

Computation

The DSC signal depends on the sample heat capacity, C_S, plus any additional heat evolved or absorbed during phase changes. After baseline subtraction, and assuming C_S to be independent of T, a first approximation to the endotherm resulting from a constant positive heating rate scan of a crystalline sample is

$$W(T) = m_S \Delta H \dot{\xi} \qquad \ldots (2)$$

(m_S is the sample mass, ΔH is the enthalpy of crystallization per unit mass and $\xi(t)$ is the proportion of the sample which has melted at time t). Given ϕ_l, the probability density function (PDF) for l, we can use equation (1) to derive a PDF for T_m, ϕ_m, such that

$$\xi(t) = \int_{T_o}^{T} \phi_m(\Theta) d\Theta \qquad \ldots (3)$$

for a test commencing at T_o, with $T = T_o + t\dot{T}$. Hence from equation (2),

$$W(T) = m_S \Delta H \dot{T} \phi_m(T) \qquad \ldots (4),$$

which implies that we can obtain $\phi_m(T)$, and hence $\phi_l(l)$, directly from W(T).

In practice, there will be a temperature difference, ΔT, between the sample temperature, T_S, and the furnace temperature, T_f, and ΔT will depend on the heating rate. Since the DSC output is generally in the form of W tabulated against T_f, one often uses some standard with a known T_m to estimate ΔT as a function of $\dot{T}_f$. When a measurement is subsequently made on a sample with an unknown T_m, T_S is then taken to be $T_f + \Delta T_{Standard}$. However, this requires the sample to have the same heat capacity as the standard (see equation (7) below), which is generally not true. More seriously, it takes no account of the effect on T_S of latent heat. To overcome these difficulties, we adapt the approach of reference 6. There must be a difference between T_S and T_f, since otherwise no heat exchange can occur between the furnace and the sample holder. Given γ, we may write

$$w(T_f) = \gamma(T_f - T_S) \qquad \ldots (5)$$

where $w(T_f)$ is the heat flow rate into the sample, and may be taken to equal $W(T_f)$ after baseline subtraction. For a thin sample undergoing melting (6),

$$\gamma(T_f - T_S) = (C_S m_S + C_p m_p)\dot{T}_S + m_S \Delta H \dot{\xi} \qquad \ldots (6),$$

where the subscripts s and p refer to the sample and the sample pan respectively. If $\dot{\xi} = 0$ (no phase change), then under steady state conditions, i.e. $\dot{T}_S = \dot{T}_f$, we have

$$\Delta T = T_f - T_S = (C_s m_s + C_p m_p)\,\dot{T}_S/\gamma = \dot{T}_S/\alpha = \dot{T}_f/\alpha \qquad \ldots (7)$$

Consider a sample with a well defined T_m. During a heating scan, equation (7) will be valid up to $T_S = T_m$, where the phase change begins (assuming no superheating). The sample will not melt instantaneously when $T_S = T_m$, but over some time interval Δt, during which T_S remains equal to T_m. Thus $\dot{T}_S = 0$, and by integrating equation (6),

$$\Delta t = (1/\alpha^2 + 2m_s\Delta H/\gamma\dot{T}_f)^{1/2} - 1/\alpha \qquad \ldots (8).$$

Thus melting will commence at $T_f = T_m + \Delta T$, and for $T_m + \Delta T < T_f < T_m + \Delta T + \dot{T}_f\Delta t$, the slope of $W(T_f)$ will be constant and equal to γ (6, 8). However, this approach becomes problematical when T_m varies within the sample, since we can no longer set $\dot{T}_S = 0$ in equation (6). Hence, we use a numerical approach, which we describe first for the case of a single well defined T_m, allowing comparison with the above analytical expressions. Rather than impose $T_S = T_m$ during melting explicitly, we assume

$$\dot{\xi} = A(T_S - T_m) \qquad \ldots (9),$$

subject to the conditions $T_S \geq T_m$ and $\xi(t) < 1$, where A is a constant, and that once it has melted, an element $d\xi$, will not resolidify. Equation (9) is merely a device to ensure that during melting, T_S remains stable with respect to fluctuations about T_m. Since the initial conditions are known, solving equation (6) for T_S with a given $\dot{T}_f$ can be carried out numerically as described in an earlier report (9). (A is chosen to be sufficiently large to keep T_S fluctuating about T_m during melting, without being so large as to require an unreasonably small final step length to obtain a stable solution.)

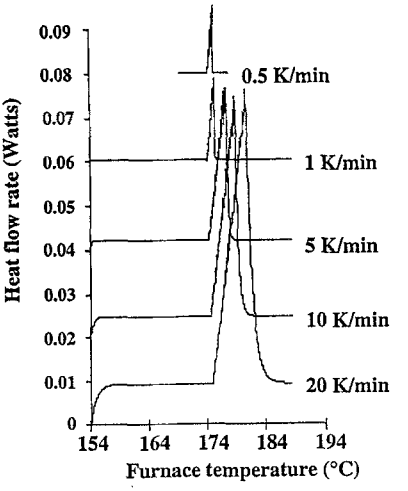

Figure 1. Calculated DSC melting peaks for a single well-defined melting point of 174 °C as a function of scanning rate.

Figure 1 shows melting peaks derived for a hypothetical material with $\Delta H = 180$ Jg^{-1}, $T_m = 174$ °C, $C_s = 2.1$ $Jg^{-1}K^{-1}$, $C_p = 0.9$ $Jg^{-1}K^{-1}$, $m_p = 28.6$ mg, $m_s = 3$ mg and $\gamma = 1.1 \times 10\text{-}2$ WK^{-1} for different scanning rates. One can verify from Figure 1 that the initial slope is equal to γ in each case, that the range of T_f over which each transition occurs is consistent with equation (8) and that the shift of the onset temperature to higher T_f as $\dot{T}_f$ is increased is consistent with equation (7).

If T_m is distributed we can replace equation (9) by assuming that the degree of conversion in an interval T_S to $T_S + \delta T_S$ (where δT_S is a discrete interval corresponding to the step length in the simulation) is given by

$$\delta\xi = \int_{T_S}^{T_S+\delta T_S} \phi_m(\Theta)d\Theta \sim \frac{\delta T_S}{2}(\phi_m(T_S + \delta T_S) + \phi_m(T_S)) \qquad \ldots (10),$$

assuming that the corresponding sample element has not already melted. This is equivalent to applying equation (10) whenever $T_S + \delta T_S > T_{Smax}$, where T_{Smax} is the maximum temperature reached previously in the sample. Since T_S will not necessarily be rising monotonically in the simulation, we must also replace the lower limit in the integral by T_{Smax}, so that

$$\delta\xi \sim \frac{T_S + \delta T_S - T_{Smax}}{2}(\phi_m(T_S + \delta T_S) + \phi_m(T_S))$$

$$\sim \frac{l(T_S + \delta T_S) - l(T_{Smax})}{2}(\phi_l((l(T_S + \delta T_S)) + \phi_l(l(T_S))) \qquad \ldots (11),$$

where $l(T)$ can be obtained from equation (1). Equation (6) is then solved as previously.

Results and Discussion

By making a reasonable *a priori* assumptions about ϕ_l, we can identify conditions appropriate to the direct determination of ϕ_l from the melting peak (assuming no recrystallization or lamellar thickening). For POM (10, 11) $T_{mo} = 200$ °C, $\Delta H = 180$ Jg^{-1}, $C_S = 2.1$ $Jg^{-1}K^{-1}$, $\sigma_e = 1.25 \times 10^{-1}$ Jm^{-2}, $\Delta h = 3.8 \times 10^8$ Jm^{-3}, and here, $C_p = 0.9$ $Jg^{-1}K^{-1}$, $m_p = 28.6$ mg and $\gamma = 1.1 \times 10^{-2}$ WK^{-1}. Given these values, we expect equation (4) to approximate well to the numerical solutions for $m_S = 3$ mg and for scanning rates below 1 K/min. In the example to be considered here, we apply equation (4) to a baseline corrected melting curve obtained for a 3.1 mg sample at 0.5 K/min, in order to estimate ϕ_m and hence ϕ_l. We insert this ϕ_l into the numerical simulation and predict the evolution of the DSC curves as a function of scanning rate for a given m_S in regimes where equation (4) is not expected to apply. The predictions can then be compared with experimental scans.

The estimated ϕ_l is shown in Figure 2. A sum of two skewed normal distributions was used to fit this data and to generate the curves shown in Figure 3, where they are compared with experimental curves for different $\dot{T}_f$. The agreement is encouraging, given that the only fitted quantity used was ϕ_l. Indeed, as long as m_S remained of the order of 3 mg, and $T_C > 150$ °C, the predicted peak positions were within 1 K of the measured peak positions. For significantly smaller m_S, there were problems with noise at very low $\dot{T}_f$, and at larger m_S (≥ 10 mg) it was difficult to reconcile high and low $\dot{T}_f$ data with the model, presumably owing to thermal gradients in the samples (6). Where good overall agreement was obtained, the shapes of the predicted curves deviated somewhat from the measured curves on the low T side of the peak. The most likely reasons for this were experimental

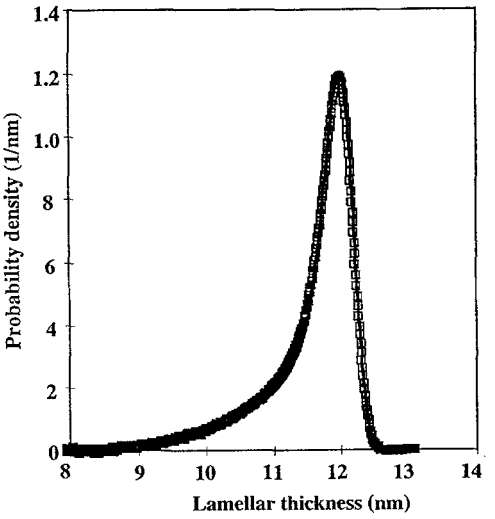

Figure 2. PDF for the lamellar thickness in POM crystallized at 153 °C derived from a melting peak obtained at a scanning rate of 0.5 K/min in a 3 mg sample. The values derived from the melting peak are open squares and the solid line is an analytical fit.

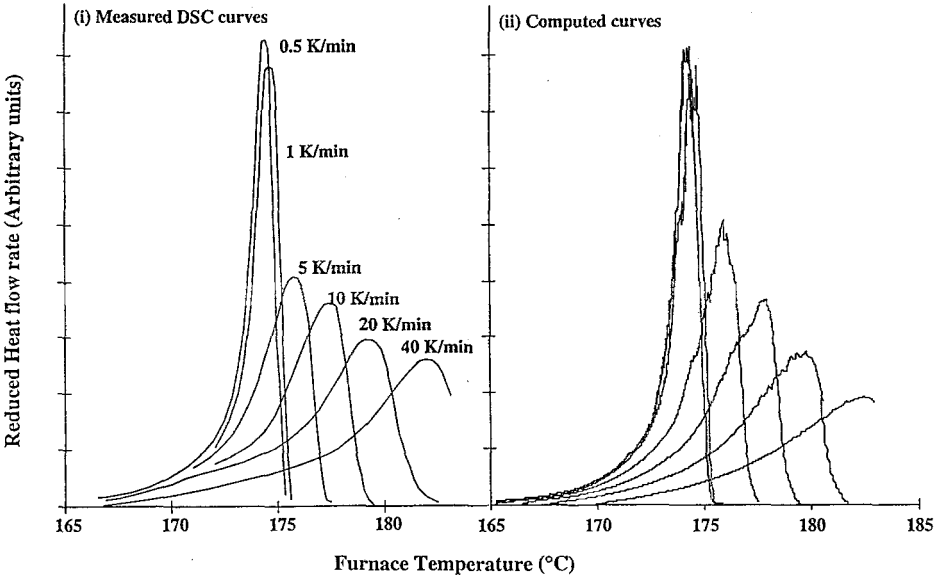

Figure 3. Heat flow rate divided by the scanning rate for a 3.1 mg sample of POM crystallized at 153 °C: (i) experimental DSC melting peaks; (ii) curves computed from Figure 2.

errors, residual recrystallization effects, an inappropriate choice of baseline and constrained melting (deviations from equation (1)). That a bimodal distribution function was necessary to fit the derived PDF might, for example, be attributable to the existence of two distinct lamellar populations. This may in turn be an artefact stemming from recrystallization during the scan of lamellae representing the extreme low l tail of the initial distribution in l. If recrystallization, or reorganization of some portion of the sample during the scan is an important factor, the effect may be suppressed at higher scanning rates, but on the other hand at higher $\dot{T}_f$ the measured curves will begin to deviate from the ideal curve in a way which is difficult to account for in terms of a simple correction procedure.

Conclusions

We have presented a numerical approach to the effect of melting point distributions on the shape of the DSC melting peak in a constant rate scan. As with earlier work on non-isothermal crystallization, experimental DSC curves obtained under well characterized conditions could be accounted for by the model. This may provide an indication of the correct experimental conditions to use when trying to derive distributions in lamellar populations from DSC data, or at the very least, an appreciation of the inadequacy of this approach. We have chosen to discuss the DSC peaks in terms of the lamellar thickness distribution since it should be possible to observe this directly by other techniques, and indeed the choice of parameters in equation (1) gives consistency between the positions of the peak maxima and SAXS and TEM data for the mean lamellar thickness (10). However, it should be stressed that the simulated curves depend only on assumptions regarding the distribution of T_m in the samples, regardless of the validity of equation (1) or of the values used here for T_{mo}, σ_e and Δh (for which there is relatively little consensus in the literature).

It has sometimes been assumed that for finite scanning rates, the measured curve can be mapped onto the ideal curve by correcting for temperature lag, and writing $T_s = T_f - W(T_f)/\gamma$ by analogy with the curves for a material with a single well-defined T_m (as in Figure 1). However it is clear from Figure 3 that such a mapping would have to involve more than transformation of the T_f axis alone, if only because the reduced curves are not all of the same height. This approach will also tend to lead to unrealistic distortion of the high T regions of the peaks. Similarly, the common practice of extrapolating the leading edge of the curves to give an onset temperature, which is taken to be the 'true melting point', is inappropriate to a material with a distributed T_m.

References

1. Wlochowicz A, Eder M (1984) Polymer 25: 1268
2. Alberola N, Cavaille JY, Perez J (1990) J. Poly. Sci. - Poly. Phys. Ed. 28: 569
3. Mills PJ, Hay JN (1984) Polymer 25: 1277
4. Darras O, Séguéla R (1993) Polymer 34: 2946
5. Lu L, Alamo RG, Mandelkern L (1994) Macromolecules 27: 6571
6. Janeschitz-Kriegl H, Wippel H, Paulik C, Eder G (1993) J. Colloid & Polym. Sci. 271: 1107
7. Sauer, BB (1994) Personal communication
8. O'Neill MJ (1964) Anal. Chem. 26: 938
9. Plummer CJG, Kausch H-H (1994) J. Colloid & Polym. Sci. 273: 227
10. Plummer CJG, Menu P, Cudré Mauroux N, Kausch H-H (1995) J. Appl. Poly. Sci. 55: 489
11. Brandrup J, Immergut EH (eds) (1989) Polymer Handbook, John Wiley, New York